Boundary-Layer Meteorology (2005) 114: 539–556

DISCUSSION AND APPLICATIONS OF SLAB MODELS OF THE CONVECTIVE BOUNDARY LAYER BASED ON TURBULENT KINETIC ENERGY BUDGET PARAMETERISATIONS

M. G. VILLANI[1,2], A. MAURIZI[1,*] and F. TAMPIERI[1]
[1]*ISAC – CNR, Via Gobetti, 101, 40129 Bologna, Italy;* [2]*Environmental Science Faculty, University of Urbino, Campus Scientifico Sogesta, 61029 Urbino, Italy*

(Received in final form 20 February 2004)

Abstract. Some of the most widely used slab model formulations for applications in the convective boundary layer are analysed and discussed. Three main classes are identified based on different approximations of the turbulent kinetic energy equation. The models appear to be quite insensitive to the initial values for boundary-layer height, and temperature discontinuity at the boundary-layer top. The slab models are applied to a case of sea-land transition from the literature, and a case of convective boundary layer time evolution over a homogeneous terrain at San Pietro Capofiume (Bologna, Italy). The different parameterisations turn out to be almost equivalent for the cases studied. The models generally underpredict the value for the height, while all give very good estimates for the mean mixed-layer temperature.

Keywords: Convective boundary layer, Entrainment velocity, Slab model, Turbulent kinetic energy equation.

1. Introduction

Thanks to the simple structure, schematic formulation and low computational cost, slab models are appealing tools for reproducing the basic and fundamental processes of the convective boundary layer (CBL). Slab models are based on the vertically integrated properties of the boundary layer. In particular, they have been implemented to study the temporal evolution of the CBL over homogeneous terrain (e.g., Tennekes, 1973; Zeman and Tennekes, 1977; Driedonks, 1982; Batchvarova and Grying, 1991, 1994; Rayner and Waston, 1991), and the spatial evolution of internal boundary layers (IBL) that results from transitions between regions with different surface characteristics (e.g., Grying and Batchvarova, 1990, 1996; Melas and Kambezidis, 1992; Källstrand and Smedman, 1997; Luhar, 1998; Batchvarova et al., 1999). Such studies (e.g., Batchvarova et al., 1999) have shown that, for convective conditions over flat terrain, the boundary-layer heights estimated by slab models are in good agreement with observations.

* E-mail: a.maurizi@isac.cnr.it

Our study examines the most widely used slab model formulations, in an attempt to distinguish substantial differences. It presents an analysis of the sensitivity to some parameters to be prescribed from data, or guessed from general information, and shows the results of two applications: a simple case of sea-land transition, and a case of CBL time evolution over a homogeneous terrain.

2. Model Formulation

Slab models are based on a very schematic representation of the atmosphere, which relies on the observed features of vertical distributions of meteorological variables characteristic of the CBL, and the free atmosphere aloft (see for example Tennekes, 1973; Tennekes and Driedonks, 1981; Fedorovich, 1995). The equations for the slab model dynamics are obtained from the Reynolds equations (the momentum balance equations and the heat equation). Considering the heat equation (the same applies for the momentum balance), the two-dimensional formulation is as follows:

$$\frac{\partial \theta}{\partial t} + u\frac{\partial \theta}{\partial x} = -\frac{\partial \overline{u'\theta'}}{\partial x} - \frac{\partial \overline{w'\theta'}}{\partial z}, \tag{1}$$

where u is the mean wind speed assumed along the x direction, θ is the mean potential temperature, $\overline{u'\theta'}$ the horizontal turbulent flux, and $\overline{w'\theta'}$ the vertical turbulent flux. In an unsteady, horizontally homogeneous CBL, where advection is neglected, the equation reduces to

$$\frac{\partial \theta}{\partial t} = -\frac{\partial \overline{w'\theta'}}{\partial z}, \tag{2}$$

and it gives the temporal evolution for θ at a fixed location. Conversely, if a steady state is considered, the heat equation (1) becomes:

$$u\frac{\partial \theta}{\partial x} = -\frac{\partial \overline{u'\theta'}}{\partial x} - \frac{\partial \overline{w'\theta'}}{\partial z}, \tag{3}$$

and it provides the spatial evolution of θ at a fixed time. Although the horizontal flux $\overline{u'\theta'}$ is generally larger than the vertical flux $\overline{w'\theta'}$ (see Monin and Yaglom, 1971, pp. 522–523), its spatial derivative has a different weight according to the region considered: it is expected to become important in the proximity of surface discontinuities, and to be negligible far away, where spatial homogeneity can be assumed. If $\frac{\partial \overline{u'\theta'}}{\partial x} \approx 0$, Equation (3) becomes equivalent to Equation (2), through the transformation $x = ut$, provided the mean wind speed u is a constant. In this case the study of the temporal evolution of a CBL over horizontal homogeneous terrain and the spatial development of an IBL, at a fixed time, and far from the surface transition,

can be treated with the same equations, through a coordinate transformation. In the discussion that follows, the slab model dynamics is presented considering the temporal CBL evolution (the case of spatial IBL growth due to a surface variation is analogous).

The momentum balance equations and the heat equation are integrated over the CBL depth to obtain the temporal evolution for the mean variables (e.g., Tennekes and Driedonks, 1981; Fedorovich, 1995). The key issue is to analyse the behaviour of the discontinuities across the boundary-layer top in the horizontal wind components, Δu and Δv, and in the potential temperature, $\Delta\theta$, i.e., the differences between the background tropospheric values of wind velocity and potential temperature estimated at the boundary-layer height, and their mean values in the boundary layer. The time evolution of these quantities is obtained from the Reynolds equations integrated over the boundary-layer depth. Turbulent fluxes at the boundary-layer height, h, are assumed to be parameterised using the equation of transport across an interface, for example $-\overline{w'u'} = \Delta u\, w_e$, where w_e is the entrainment vertical velocity and $\overline{w'u'}$ is the momentum flux. The entrainment vertical velocity is defined from the continuity equation as

$$w_e = \frac{dh}{dt}, \tag{4}$$

where subsidence is neglected (see Stull, 1988). The resulting system of differential equations represents the slab model dynamics (see also Tennekes and Driedonks, 1981; Driedonks, 1982; Fedorovich, 1995):

$$\frac{d\Delta\theta}{dt} = \Gamma w_e - \frac{\overline{w'\theta'}_s}{h} - \frac{\Delta\theta}{h} w_e, \tag{5}$$

$$\frac{d\Delta u}{dt} = S_x w_e + f\Delta v - \frac{\overline{w'u'}_s}{h} - \frac{\Delta u}{h} w_e, \tag{6}$$

$$\frac{d\Delta v}{dt} = S_y w_e - f\Delta u - \frac{\overline{w'v'}_s}{h} - \frac{\Delta v}{h} w_e, \tag{7}$$

where $\Delta\theta$, Δu, and Δv are the discontinuities in potential temperature and horizontal wind components u and v, respectively, across the boundary-layer top, h; $\Gamma = \frac{\partial\theta}{\partial z}$, $S_x = \frac{\partial u}{\partial z}$, $S_y = \frac{\partial v}{\partial z}$ are the vertical gradients for potential temperature and wind components respectively in the free atmosphere above the boundary layer; f is the Coriolis parameter, and $\overline{w'\theta'}_s$, $\overline{w'u'}_s$, and $\overline{w'v'}_s$ are the turbulent fluxes at the surface.

To solve the system, the vertical gradients Γ, S_x, and S_y, and the surface turbulent fluxes must be prescribed, and an expression for the entrainment velocity w_e is required. Suitable parameterisations for this velocity are derived from the turbulent kinetic energy ($\bar{e}$) equation evaluated at the interface

(for a review, see Zilitinkevich et al., 1979; Tennekes and Driedonks, 1981). The $\bar{e}$ equation is

$$\frac{d\bar{e}}{dt} = \frac{g}{\Theta}\overline{w'\theta'} - \overline{w'u'}\frac{\partial u}{\partial z} - \overline{w'v'}\frac{\partial v}{\partial z} - \frac{\partial}{\partial z}\left(\overline{w'e'} + \frac{\overline{w'p'}}{\rho}\right) - \varepsilon, \tag{8}$$

where p' is the pressure fluctuation, ρ is the air density, and ε is the dissipation rate of turbulent kinetic energy.

The terms are as follows:

- $\frac{d\bar{e}}{dt}$ provides the local storage or tendency of $\bar{e}$. Assuming that the increase of turbulent energy near the level h is associated with turbulent mixing of entrained air, Zilitinkevich (1975) supposed $\bar{e} \sim \sigma_w^2$, where σ_w^2 is the variance of the vertical velocity in the bulk of the CBL, and hypothesised the existence of the timescale $\left(\frac{1}{h}\frac{dh}{dt}\right)^{-1}$, leading to $\frac{d}{dt}\bar{e} \sim \frac{\bar{e}}{h}\frac{dh}{dt} \sim \frac{\sigma_w^2}{h}w_e$ Zilitinkevich (1975) and Zilitinkevich et al. (1979) suggested that $\frac{d\bar{e}}{dt}$ needs to be taken into account when temporal changes are rapid and the inversion strength is small, a condition that generally occurs at initial time when the free atmosphere is weakly stratified.
- $\frac{g}{\Theta}\overline{w'\theta'}$ is the buoyant production or consumption term. The temperature at the surface T_s is used instead of Θ, and the sensible heat flux at the boundary-layer top is by definition $-\overline{w'\theta'} = \Delta\theta\, w_e$ (e.g., Tennekes and Driedonks, 1981; Driedonks, 1982).
- $-\overline{w'u'}\frac{\partial u}{\partial z}$ and $\overline{w'v'}\frac{\partial v}{\partial z}$ are the shear production terms. The turbulent fluxes at h are $-\overline{w'u'} = \Delta u\, w_e$, and $-\overline{w'v'} = \Delta v\, w_e$. According to Tennekes and Driedonks (1981) and Driedonks (1982) the gradients are estimated through $\frac{\partial u}{\partial z} \approx \frac{\Delta u}{\tilde{d}}$, $\frac{\partial v}{\partial z} \approx \frac{\Delta v}{\tilde{d}}$. Here, $\tilde{d}$ is the undetermined effective depth of the entrainment layer that some authors (e.g., Pollard et al., 1973; Tennekes and Driedonks, 1981) have substituted with h.
- $\frac{\partial}{\partial z}\left(\overline{w'e'} + \frac{\overline{w'p'}}{\rho}\right)$ represents the turbulent transport of $\bar{e}$, and the pressure correlation term, respectively. These terms are often assumed to be proportional to $\frac{\sigma_w^3}{h}$ (see Tennekes, 1973). The expression comes from a dimensional balance between the flux convergence of kinetic energy and the downward heat flux, in an idealised situation where the $\bar{e}$ equation is steady, and wind shear and viscous dissipation are ignored. Generally, it is assumed that σ_w is given by an interpolation between the convective velocity w_*, and the friction velocity u_*. Here, $\sigma_w^3 = w_*^3 + \eta^3 u_*^3$, where η is an empirical constant, whose value is usually close to 2.
- ε is the dissipation of $\bar{e}$. Zeman and Tennekes (1977) suggest that $\varepsilon \approx \sigma_w^2 N$, where $N = (g\Gamma/\Theta)^{1/2}$ is the Brunt–Väisälä frequency. This parameterisation is obtained by assuming that the energy produced by the turbulent structures is locally dissipated against the stable stratification.

TABLE I

Values for the empirical constants c_1, c_2, c_3, c_4 used in the parameterisation of the turbulent kinetic energy equation. TE73 refers to the Tennekes (1973) parameterisation, ZI75 to Zilitinkevich (1975), ZT77 to Zeman and Tennekes (1977), and TD81 to Tennekes and Driedonks (1981).

Author	c_1	c_2	c_3	c_4
TE73	0.2	–	–	–
ZI75	0.2	1.5	–	–
ZT77	0.6	4.3	0.03	–
TD81	0.6	4.3	0.03	0.7

The general form of the parameterised $\bar{e}$ equation considered in this study is therefore:

$$c_2 \frac{\sigma_w^2}{h} w_e = -\frac{g}{T}\Delta\theta w_e + c_4 \frac{|\Delta u|^2}{h} w_e + \frac{c_1}{h}\sigma_w^3 - c_3 \sigma_w^2 N, \tag{9}$$

where c_1, c_2, c_3, and c_4 are empirical constants, whose values are commonly set to compensate the inclusion or exclusion of the other terms in the $\bar{e}$ equation (see Table I). Many authors (e.g., Tennekes, 1973; Zilitinkevich, 1975; Zeman and Tennekes, 1977; Tennekes and Driedonks, 1981) have referred to Equation (9), choosing simplified expressions to close the system of differential equations (5), (6), and (7). Some of the most common parameterisations adopted will be presented herein.

Two main classes of models can be distinguished according to whether the $\bar{e}$ equation is steady $\left(\frac{d\bar{e}}{dt} = 0\right)$ or not $\left(\frac{d\bar{e}}{dt} \neq 0\right)$. One model representative of the former class is proposed by Tennekes (1973). In the $\bar{e}$ equation, this author considers the buoyancy and the flux divergence terms, which, assuming $\frac{d\bar{e}}{dt} = 0$, are in balance. In the unsteady class, several models can be identified, which differ in the values chosen for the empirical constants present in Equation (9). One group of models uses a formulation for the $\bar{e}$ equation that includes the buoyancy and the flux divergence terms (e.g., Zilitinkevich, 1975; Driedonks, 1982; Gryning and Batchvarova, 1990; Melas and Kambezidis, 1992; Källstrand and Smedman, 1997; Luhar, 1998). Among them, Gryning and Batchvarova (1990) parameterise the rate of change for $\bar{e}$ as $\frac{d\bar{e}}{dt} \sim \frac{u_*^2}{h} w_e$. However, the use of the friction velocity, u_*, is not justified, and it does not represent the correct scale for the CBL. Moreover, since $\frac{u_*}{\sigma_w} \ll 1$, this parameterisation reduces to that of Tennekes (1973). Another group of models takes into account also the dissipation term in Equation (9) (e.g., Zeman and Tennekes, 1977; Driedonks, 1982).

A restricted number of models (e.g., Zeman and Tennekes, 1977; Tennekes and Driedonks, 1981; Driedonks, 1982) add the shear term of Equation (9),

TABLE II
Summary of the terms considered in the turbulent kinetic energy equation by the different authors.

Author	$\left(\frac{d\bar{e}}{dt}\right)$	$\frac{g}{T_s}\overline{w'\theta'}$	$-\overline{w'u_i'}\frac{\partial u_i}{\partial z}$	$-\frac{\partial}{\partial z}\left(\overline{w'e'}+\frac{\overline{w'p'}}{\rho}\right)$	ε	w_e
TE73	–	Yes	–	Yes	–	$\frac{\frac{c_1}{h}\sigma_w^3}{\frac{g}{T}\Delta\theta}$
ZI75	Yes	Yes	–	Yes	–	$\frac{\frac{c_1}{h}\sigma_w^3}{\frac{g}{T}\Delta\theta+\frac{c_2}{h}\sigma_w^2}$
ZT77	Yes	Yes	–	Yes	Yes	$\frac{\frac{c_1}{h}\sigma_w^3-c_3\sigma_w^2 N}{\frac{g}{T}\Delta\theta+\frac{c_2}{h}\sigma_w^2}$

in the above mentioned form. However, as the shear term is estimated using h as the vertical length scale for velocity variations, it becomes smaller than the other contributions with increasing h. Thus, this parameterisation turns out to be equivalent to the formulations that only consider buoyancy, the flux divergence terms and dissipation. Recent studies on the entrainment zone evolution (e.g., Fedorovich and Thater, 2001; Fedorovich et al., 2001; Kim et al., 2003) have suggested that the shear term in the $\bar{e}$ equation could play a major role in turbulent kinetic energy production. Therefore, better parameterisations for the shear contribution could constitute a significant improvement for the model formulation.

As a result of the analysis, only three kinds of models can be considered substantially different, and they are given by Equations (4), (5), and (9) with $c_4 = 0$. The parameterisations from Tennekes (1973) (here after TE73: steady), Zilitinkevich (1975) (ZI75: unsteady, no dissipation), Zeman and Tennekes (1977) (ZT77: unsteady, dissipation) were chosen in the present study as being representative of the three kinds. Since they provide different formulations for the entrainment velocity, they are referred to herein as the w_e models. Table II provides a summary of the expressions adopted.

3. Slab Model Results

3.1. Sensitivity analysis

In the present slab model implementation, mean surface temperature values, the vertical gradient of temperature at the beginning of the growth (or upstream of the discontinuity), and the surface fluxes can be derived from data or from larger scale numerical simulations. In general, the vertical gradients of temperature are not constant with height, and surface fluxes are not constant in time (if time growth of the CBL is considered over homogeneous terrain) or not uniform in space (if the IBL growth past a discontinuity is described). The present formulation presupposes the existence of a local equilibrium, namely that variations occur on scales larger than the relevant turbulent scales of mixing. The numerical formulation of the model allows one to deal with variable gradient and fluxes, in order to give a more realistic evolution of the boundary layer.

To allow the solution of the set of differential Equations (4), (5), with Equation (9), the initial values for $\Delta\theta$, and h ($\Delta\theta_{\text{in}}$, h_{in}, respectively) are needed. These values are difficult to obtain or measure, so that commonly they are set arbitrarily. To evaluate the effects of the choice, taking the TE73, ZI75, and ZT77 expressions, simulations were conducted, varying the values for the initial height h_{in}, and the discontinuity in temperature $\Delta\theta_{\text{in}}$. The values of the variables considered are reported in Table III.

TABLE III

Values for the variables used in the sensitivity analyses performed on the TE73, ZI75, and ZT77 parameterisations for w_e. The sign (*) indicates values not applied for TE73.

	Γ (K m^{-1})	h_{in} (m)	$\Delta\theta_{in}$ (K)	$\overline{\theta' w'}\|_s$ (K m s^{-1})	u_* (m s^{-1})	T_0 (K)
Sensitivity to Γ	1e−3	20	0.5	0.3	0.6	295
	5e−3	20	0.5	0.3	0.6	295
	1e−2	20	0.5	0.3	0.6	295
	5e−2	20	0.5	0.3	0.6	295
Sensitivity to h_{in}	1e−3	0.1*	1	0.3	0.6	295
	1e−3	5*	1	0.3	0.6	295
	1e−3	10	1	0.3	0.6	295
	1e−3	50	1	0.3	0.6	295
	1e−3	100	1	0.3	0.6	295
Sensitivity to $\Delta\theta_{in}$	1e−3	20	0.05*	0.3	0.6	295
	1e−3	20	0.5	0.3	0.6	295
	1e−3	20	1	0.3	0.6	295
	1e−3	20	5	0.3	0.6	295

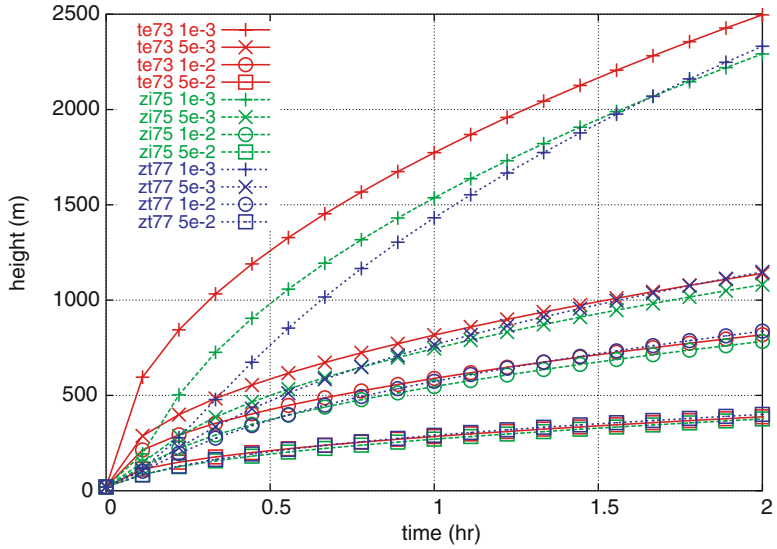

Figure 1. Sensitivity of TE73, ZI75 and ZT77 models to the vertical gradient of potential temperature Γ. Here, h_{in} and $\Delta\theta_{in}$ were set at 20 m, and 0.5 K, respectively. Each line represents the height resulting from the w_e models using various values for Γ (expressed in K m^{-1}).

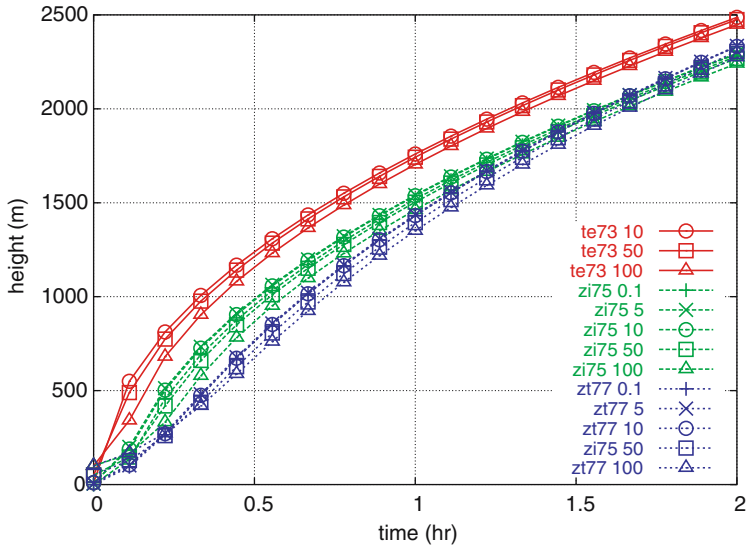

Figure 2. Sensitivity of TE73, ZI75 and ZT77 models to the initial height h_{in}. $\Delta\theta_{\text{in}}$ was set at 1 K. Each line represents the height resulting from the w_e models using various values for h_{in} (expressed in m).

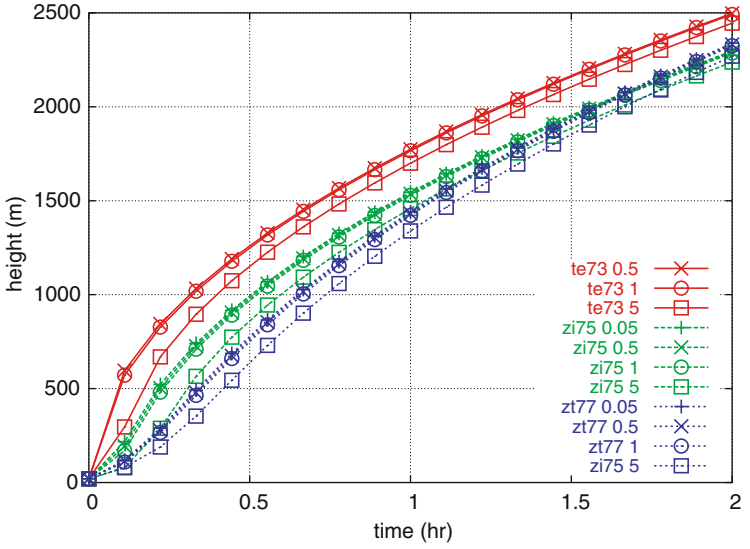

Figure 3. Sensitivity of TE73, ZI75 and ZT77 models to $\Delta\theta_{\text{in}}$. Here, h_{in} was set at 20 m. Each line represents the height resulting from the w_e models using various values for $\Delta\theta_{\text{in}}$ (expressed in K).

The parameter Γ, which provides a measure of the stratification aloft, represents the dominant factor in determining the CBL height (see Figure 1). Weak atmospheric stratification, typically $\Gamma \approx 0.001\,\mathrm{Km}^{-1}$ characteristic of summertime conditions, makes h grow rapidly. The various parameterisations for w_e produce estimates for h, which are more different at the beginning of the simulation ($\delta h \approx 85\%$, where δh represents the relative h variations among the w_e models), and closer at the end of the simulation ($\delta h \approx 8\%$). Heights have values generally greater for TE73, and smaller for ZT77, because of the lower values for w_e provided by the ZT77 parameterisation. Large temperature gradients, $\Gamma \approx 0.02\,\mathrm{Km}^{-1}$ generally found in wintertime, limit the CBL growth and the differences in h at the beginning of the simulations.

The study on model sensitivity to h_{in} and $\Delta\theta_{\mathrm{in}}$ was performed by choosing a weak atmospheric stratification ($\Gamma = 0.001\,\mathrm{Km}^{-1}$). Variations of even one order of magnitude in h_{in} produce $\delta h \approx 50\%$ at $h \sim 250\,\mathrm{m}$, which eventually diminishes to less than 3% at about 2000 m (Figure 2). The same behaviour was found for the sensitivity study on $\Delta\theta_{\mathrm{in}}$ (Figure 3), where h shows small variations for $\Delta\theta_{\mathrm{in}}$ ranging between 0.05 and 1 K. The CBL height was generally much lower when the value 5 K was chosen for $\Delta\theta_{\mathrm{in}}$. This represents a potential temperature discontinuity at the entrainment zone, characteristic of a very well-developed mixed layer, which is generally found at noon. It is therefore rarely encountered during the morning boundary-layer development. This analysis suggests that the model is 'robust' in most realistic cases, especially if results are considered at $t \gg t_0$, the initial time, or at distances far from the surface transition. The values for h_{in} and $\Delta\theta_{\mathrm{in}}$ chosen for the studies presented in the following sections are given in Table IV.

3.2. A STUDY OF SEA-LAND TRANSITION

It is of interest to compare the different w_e models in predicting the spatial growth of an internal boundary layer in steady conditions, and the temporal growth of the horizontally homogeneous mixed layer under a temperature

TABLE IV
Initial values for h and $\Delta\theta$ chosen for TE73, ZI75, and ZT77 parameterisations.

Model	h_{in} (m)	$\Delta\theta_{in}$ (K)
TE73	20	0.5
ZI75	10	0.5
ZT77	10	0.5

inversion. In this subsection the slab model is implemented in the case-study of spatial internal boundary-layer evolution represented by a sea-land transition. Among the studies reported in the literature on this topic, the work by Gryning and Batchvarova (1990) was chosen as a reference case, since it provides a complete dataset for testing, and proposes an analytical model based on a combination of the TE73 and ZI75 expressions for the $\bar{e}$ equation (see Gryning and Batchvarova (1990), for more details). For more accurate descriptions of this work and the observations collected, see Gryning and

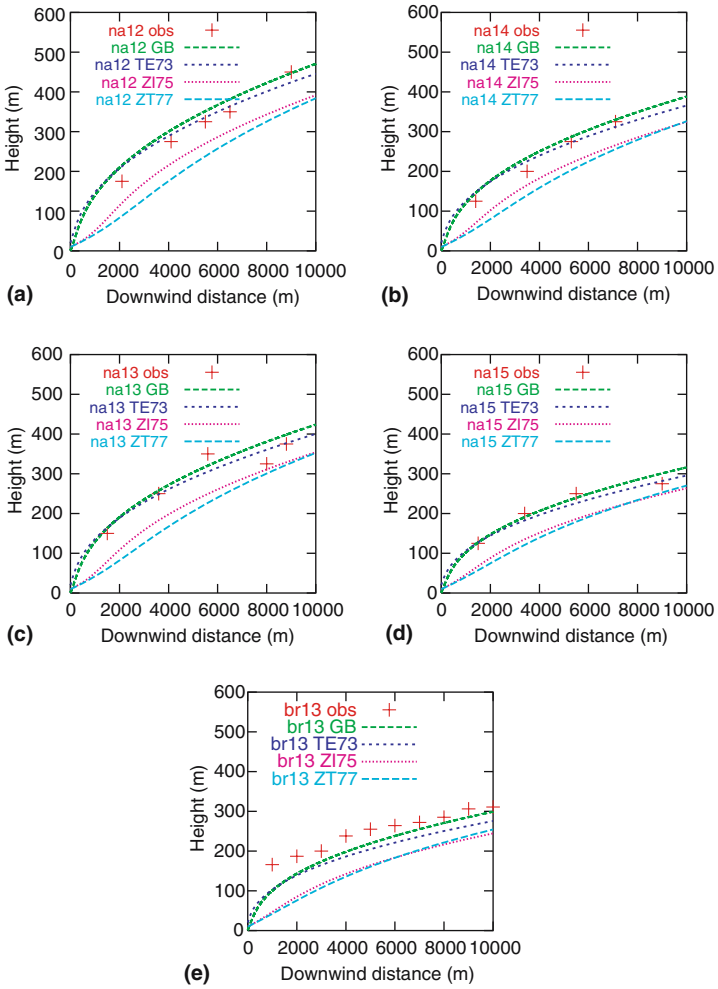

Figure 4. The sea-land transition from data of the Nanticoke (indicated as na: na12, na13, na14, na15) and Brookhaven (in the legend br: br13) experiments. Plus signs stand for the observations. The letters 'GB' show results from the Gryning and Batchvarova model. Different dashed and dotted lines are the height space-evolutions obtained with the w_e models.

Batchvarova (1990), Portelli (1982), Raynor et al. (1979), Steyn and Oke (1982), Stunder and SethuRaman (1985). In the present study, the observations from the Nanticoke (at 1200, 1300, 1400, 1500 LST) and Brookhaven (at 1330 EST) experiments were considered. Both the experiments provided spatially uniform values for potential temperature vertical gradients, surface fluxes and mean wind velocity.

The results obtained with the different w_e for the growth of the coastal internal BL are presented in Figure 4. For the cases analysed, the simplest parameterisation for w_e, given by TE73, provided the closest estimates for the height h to the observations. Moreover, for the Nanticoke cases at 1200, 1300, 1400, and 1500 LST, TE73 seems to perform even better than the analytical model used by Gryning and Batchvarova. The models for ZI75 and ZT77 underestimated h in all cases. The introduction of the rate of change of $\bar{e}$ (Table II) seems to determine a smaller w_e, which provides a 'slower' h growth. Here, besides the Brookhaven 1330 EST case where all models underestimated the internal boundary-layer height, the cases analysed are better fitted by the most simple w_e expression, which is based on the steady formulation of the $\bar{e}$ equation.

3.3. A STUDY OF TEMPORAL BOUNDARY-LAYER GROWTH

The slab model was applied to the analysis of the temporal growth of the horizontally homogeneous mixed layer, using summer and winter observations collected at San Pietro Capofiume (Lat 44.65 N, Lon 11.62 E), 25 km north from Bologna (Italy). The site is about 11 m a.s.l., in a flat rural location and is representative for the area (Bonafé, 2003, personal communications. See also Deserti et al., 2003, for a more detailed description of the site and experiments performed). Half hourly values of sensible heat and momentum fluxes were available from anemometric measurements collected at 10 and 2.9 m a.g.l., during summer and winter, respectively. Measurements from radiosondes provided vertical profiles of temperature, wind speed and wind direction at 0000 and 1200 LST each day (at San Pietro Capofiume, LST = GMT + 1 hr). Surface temperature values were also available from a meteorological station located at the site. Examining the diurnal cycle for sensible heat, surface temperature, radiation, and excluding the rain periods, the following days were chosen as representative of idealised convective conditions for the slab model application: 11, 13, 14, 24, 25, 26 July 2001; and 22 and 31 January 2002 (31 January is less representative of convective conditions than the other days, as radiometric and sensible heat measurements suggested a cloudy sky during the day).

For each selected day, the boundary-layer growth was simulated from 'sunrise', determined as the time when the sensible heat flux started to have

positive values, to noon. Time dependent surface temperature, sensible heat and momentum fluxes were introduced in the model. These quantities were interpolated using the Akima cubic spline interpolation (Akima, 1978), which minimises oscillations between the values. The potential temperature profile at 0000 LST was used to determine the vertical gradient of potential temperature, Γ, characteristic of the air capping the mixed-layer height during the boundary-layer development. Here, Γ was assumed to be independent of time, because observed synoptic conditions do not change rapidly. Since Γ is the main factor in determining the h growth, care was taken to define a point value for Γ that takes into account the h time evolution and, thus, the stratification of the layers of air above the mixed-layer height. With this aim in mind, Γ was calculated at each height by linearly interpolating between the Γ value at the h just reached, and the value for the layer immediately aloft.

From the simulations performed, mixed-layer potential temperatures, θ_{cbl}, were calculated as $\theta_{\mathrm{cbl}} = \theta_{00}(h) - \Delta\theta$, where $\theta_{00}(h)$ is the potential temperature at h according to the 0000 LST temperature profile, and $\Delta\theta$ is the discontinuity in θ predicted by the slab model. These quantities were compared to the observed mean temperatures, which were obtained by averaging the 1200 LST temperature profiles up to the estimated h. This height was empirically determined as an average value between the two levels, where the noon potential temperature showed the step-like trend related to the entrainment zone.

The values for h and mixed-layer temperatures obtained at noon from the TE73, ZI75, and ZT81 models, were plotted over the potential temperature profile at 1200 LST, giving an indication of the 'goodness' of the h and mean temperatures simulated. Estimated boundary-height values from the mass-consistent meteorological pre-processor CALMET (Scire et al., 2000) were also available for 1200 LST (Deserti et al., 2001), allowing a further comparison with the slab model results. In convective conditions CALMET provides estimates for the mixed-layer height, based on the knowledge of surface sensible heat fluxes, temperature profiles, and on the empirical expression of Venkatram (1980), valid for neutral boundary layer (Scire et al., 2000).

Figure 5 shows two case-studies on the time evolution of the height h of one day during summertime (a), and one during wintertime (b). The results are summarised in Figures 6 and 7, which show how the simulated values for h and the mean mixed-layer temperatures compare with the observations.

A general overview of the scatterplot for h, Figure 6, shows that in most of the cases analysed, the w_e models and CALMET provide estimated h close to the observed values. Compared to the w_e models, the CALMET h values are usually overestimated for the summer cases, and underestimated for the winter ones. The w_e models underpredict h in the majority of the cases. Moreover, unlike the h spatial evolution analysis in 3.2, it is difficult here to establish whether the assumption of a steady $\bar{e}$ equation works better than the

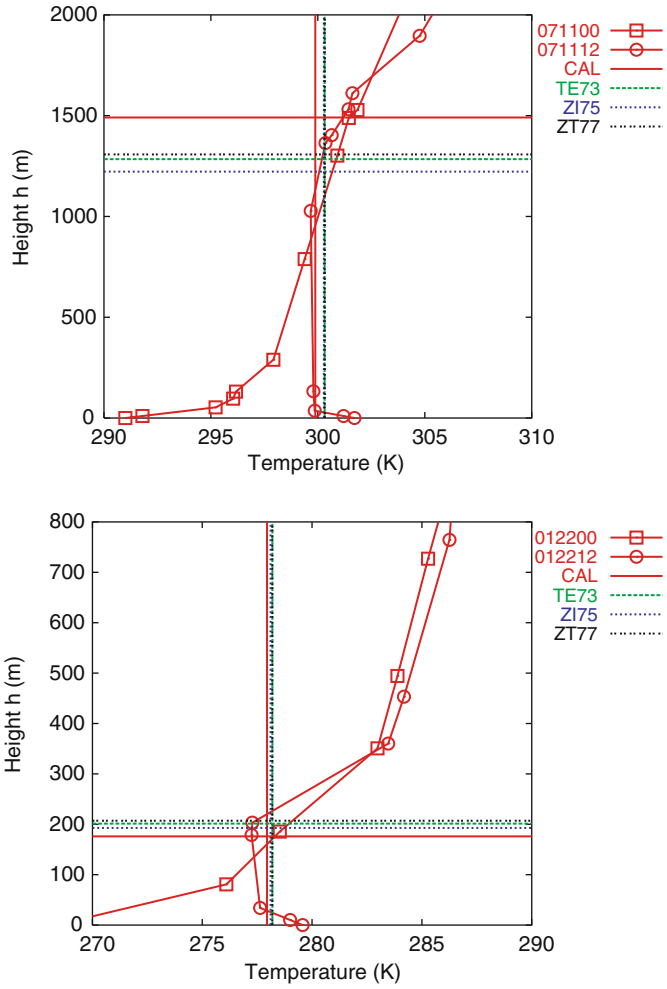

Figure 5. Representation of two time evolution cases at San Pietro Capofiume: simulation for 11 July 2001 (upper panel); simulation for 22 January 2002 (lower panel). The solid lines represent the potential temperature profiles at 0000 LST (squared points), and at noon (circled-points). The horizontal lines are the boundary-layer heights reached at noon by CALMET (CAL) and the three w_e models. The vertical lines represent the mixed-layer potential temperature values calculated from the temperature profile at 1200 LST (solid line) and the ones predicted by the models (which have the same line-style as the boundary-layer heights from the various models).

non steady hypothesis. Among the models considered, the ZT77 and TE73 usually give more correct height values, while h is generally underestimated in ZI75.

The mean potential temperatures predicted by the models fit the observed mean temperatures much better than in the case of h (Figure 7). The model estimates are all very similar and close to the observations.

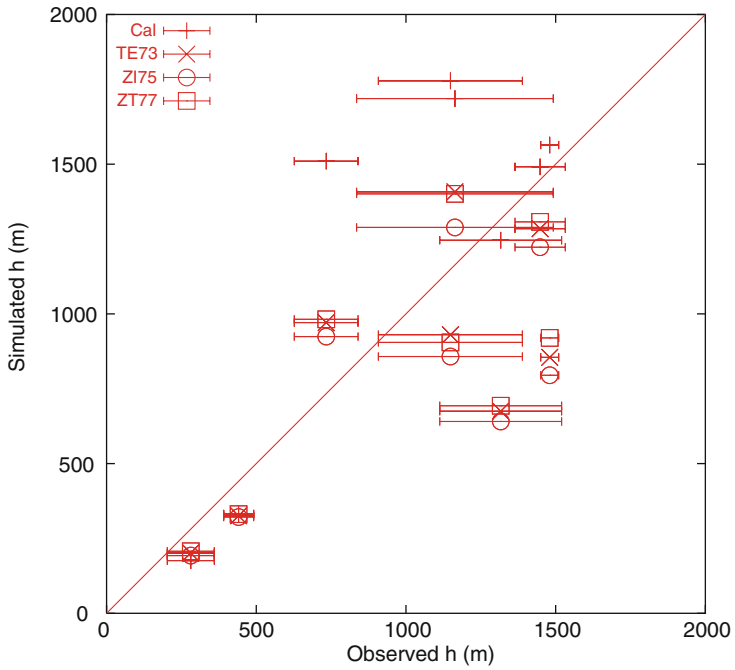

Figure 6. Scatterplot of observed versus simulated boundary-layer heights at noon, at San Pietro Capofiume. The horizontal bars represent estimated errors for h, and were determined as the levels where the vertical profile of potential temperature changes from the typical constant values in the mixed layer to increasing values in the stratified air aloft. The winter cases are located at the bottom left part of the plot.

It is interesting to observe that the days with better predicted mean temperatures are not necessarily the same days giving the best estimates of h. Reasons for different precision and lack of correlation in producing correct values for the variables probably arise from the methods adopted. In particular, the integration process applied to the observed temperature profiles provides a very robust value for the mean quantities, since errors in the observations can be more easily levelled off. The h estimation, on the other hand, relies on the subjective choice of single points in the observed temperature profile.

4. Conclusions

The analyses performed provided the following conclusions.

– Several slab models can be distinguished in the literature for CBL studies; among them, three kinds are selected as substantially different models. One of them is based on the steady formulation of the $\bar{e}$ equation. The other

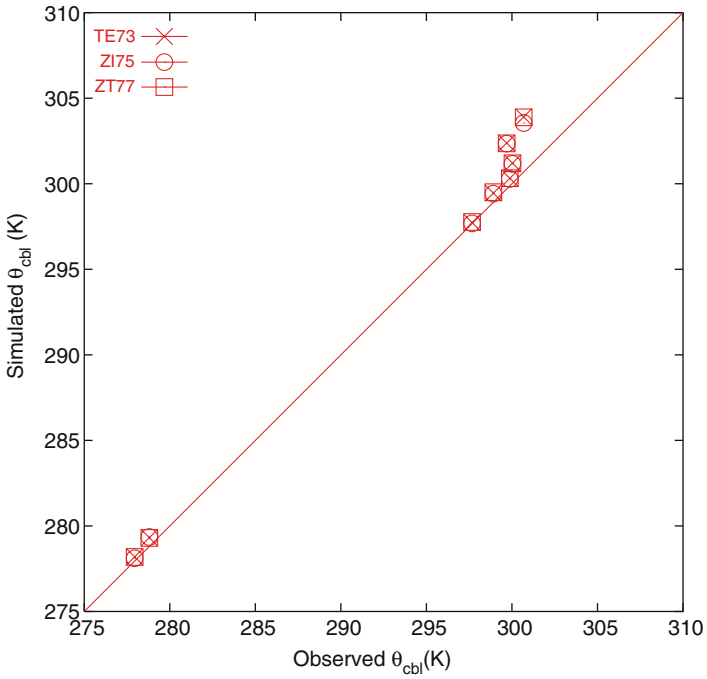

Figure 7. Scatterplot of observed versus simulated mixed-layer potential temperatures at noon, at San Pietro Capofiume. As for the boundary-layer heights comparison, the winter cases are located at the bottom left part of the plot.

two models, for which $\frac{d\bar{e}}{dt} \neq 0$, differ by including or omitting the dissipation term in the $\bar{e}$ equation.

– The stratification of the air above the mixed layer represents the key factor in determining the boundary-layer development. Therefore, particular care should be taken in prescribing the vertical potential temperature gradients.
– In the boundary-layer height time-evolution study, it is not easy to define which w_e model works best. The models generally underpredict the boundary-layer height, though all give a very good estimate for the mean mixed-layer temperature.

The positive outcomes of this study and similar analyses in the literature suggest that slab models could be applied to improve operational model performances. In particular, subgrid heterogeneities represented by areas with different surface features would be ideal situations for slab model implementions. Better estimates of the internal boundary-layer height could produce more accurate values for the grid-averaged meteorological variables required by the operational models, such as turbulent fluxes.

Acknowledgements

The authors would like to thank Marco Deserti and Giovanni Bonafé for providing the observations at San Pietro Capofiume and the CALMET results. This work was partially supported by the EC contract EUG2/2000/00522 (EURAINSAT Project).

References

Akima, H.: 1978, 'A Method of Bivariate Interpolation and Smooth Surface Fitting for Irregularly Distributed Data Points', *ACM Trans. Math. Software* **4**, 148–159.

Batchvarova, E. and Gryning, S. E.: 1991, 'Applied-Model for the Growth of the Daytime Mixed Layer', *Boundary-Layer Meteorol.* **56**, 251–274.

Batchvarova, E. and Gryning, S. E.: 1994, 'An Applied-Model for the Height of the Daytime Mixed-Layer and the Entrainment Zone', *Boundary-Layer Meteorol.* **71**, 311–323.

Batchvarova, E., Cai, X. M., Gryning, S. E., and Steyn, D.: 1999, 'Modelling Internal Boundary-Layer Development in a Region with a Complex Coastline', *Boundary-Layer Meteorol.* **90**, 1–20.

Deserti, M., Bonafé, G., Minguzzi, E., Tagliazucca, M., and Trivellone, G.: 2003, 'The Urban Atmospheric Boundary Layer: Experimental Campaigns in Bologna (Italy)', in: S. Sokhi and J. Brechler (eds.), *Proceedings of the 4th International Conference on Urban Air Quality. Measurements, Modelling and Management, Prague, 25–27 March 2003*, pp. 404–407.

Deserti, M., Cacciamani, C., Golinelli, M., Kerschbaumer, A., Leoncini, G., Savoia, E., Selvini, A., Paccagnella, T., and Tibaldi, S.: 2001, 'Operational Meteorological Pre-Processing at Emilia-Romagna ARPA Meteorological Service as a Part of a Decision Support System for Air Quality Management', in P. A. Coppalle (ed.), *Proceedings of the Sixth Workshop on Harmonization within Atmospheric Dispersion Modelling for Regulatory Purposes*; *Int. J. Environ. Pollut.* **16**, (1–6).

Driedonks, A. G. M.: 1982, 'Models and Observations of the Growth of the Atmospheric Boundary Layer', *Boundary-Layer Meteorol.* **23**, 283–306.

Fedorovich, E.: 1995, 'Modeling the Atmospheric Convective Boundary Layer within a Zero-Order Jump Approach: An Extended Theoretical Framework', *J. Appl. Meteorol.* **34**, 1916–1928.

Fedorovich, E. and Thater, J.: 2001, 'Vertical Transport of Heat and Momentum across a Sheared Density Interface at the Top of a Horizontally Evolving Convective Boundary Layer', *J. Turbulence* **2**, 1–17.

Fedorovich, E., Nieuwstadt, F. T. M., and Kaiser, R.: 2001, 'Numerical and Laboratory Study of Horizontally Evolving Convective Boundary Layer Part II: Effects of Elevated Wind Shear and Surface Roughness', *J. Atmos. Sci.* **58**, 546–560.

Gryning, S. E. and Batchvarova, E.: 1990, 'Analytical Model for the Growth of the Coastal Internal Boundary Layer during Onshore Flow', *Quart. J. Roy. Meteorol. Soc.* **116**, 187–203.

Gryning, S. E. and Batchvarova, E.: 1996, 'A Model for the Height of the Internal Boundary Layer over an Area with an Irregular Coastline', *Boundary-Layer Meteorol.* **78**, 405–413.

Källstrand, D. and Smedman, A.: 1997, 'A Case Study of the Near-Neutral Coastal Internal Boundary-Layer Growth: Aircraft Measurements Compared with Different Model Estimates', *Boundary-Layer Meteorol.* **85**, 1–33.

Kim, S. W., Park, S., and Moeng, C. H.: 2003, 'Entrainment Processes in the Convective Boundary Layer with Varying Wind Shear', *Boundary-Layer Meteorol.* **108**, 221–245.

Luhar, A. K.: 1998, 'An Analytical Slab Model for the Growth of the Coastal Thermal Internal Boundary Layer under Near-Neutral Onshore Flow Conditions', *Boundary-Layer Meteorol.* **88**, 103–120.

Melas, D. and Kambezidis, H. D.: 1992, 'The Depth of the Internal Boundary Layer over an Urban Area Under Sea-Breeze Conditions', *Boundary-Layer Meteorol.* **61**, 247–264.

Monin, A. S. and Yaglom, A. M.: 1971, *Statistical Fluid Mechanics: Mechanics of Turbulence,* Vol. 1, The MIT Press, Cambridge, MA, 769 pp.

Pollard, R. T., Rhines, P. B., and Thompson R. O. R. Y.: 1973, 'The Deepening of the Wind-Mixed Layer', *Geophys. Fluid Dyn.* **3**, 381–404.

Portelli, R. V.: 1982, 'The Nanticoke Shoreline Diffusion Experiment, June 1978 – I. Experimental Design and Program Review', *Atmos. Environ.* **16**, 413–421.

Rayner, K. N. and Watson, I.: 1991, 'Operational Prediction of Daytime Mixed Layer Heights for Dispersion Modelling', *Atmos. Environ.* **25a**, 1427–1436.

Raynor, G. S., SethuRaman, S., and Brown R. M.: 1979, 'Formation and Characteristics of Coastal Internal Boundary Layers during Onshore Flow', *Boundary-Layer Meteorol.* **16**, 487–514.

Scire, J. S., Robe, F. R., Fernau, M. E., and Yamartino, R. J.: 2000, *A User's Guide for the CALMET Meteorological Model* (*Version 5*), Earth Tech, Inc, 196 Baker Avenue, Concord, MA 01742.

Steyn, D. G. and Oke, T. R.: 1982, 'The Depth of the Daytime Mixed Layer at Two Coastal Sites: a Model and its Validation', *Boundary-Layer Meteorol.* **24**, 161–180.

Stull, R. B.: 1988, *An Introduction to Boundary Layer Meteorology*, Kluwer Academic Publishers, Dordrecht, 666 pp.

Stunder, M. and SethuRaman, S.: 1985, 'A Comparative Evaluation of the Coastal Internal Boundary-Layer Height Equation', *Boundary-Layer Meteorol.* **32**, 177–204.

Tennekes, H.: 1973, 'A Model for the Dynamics of the Inversion above a Convective Boundary Layer', *J. Atmos. Sci.* **30**, 558–567.

Tennekes, H. and Driedonks, A. G. M.: 1981, 'Basic Entrainment Equations for the Atmospheric Boundary Layer', *Boundary-Layer Meteorol.* **20**, 515–531.

Venkatram, A.: 1980, 'Estimation of Turbulence Velocity Scales in Stable and Unstable Boundary Layer for Dispersion Applications', in *Eleventh NATO-CCMS International Technical Meeting on Air Pollution Modeling and its Application*, pp. 54–56.

Zeman, O. and Tennekes, H.: 1977, 'Parameterization of the Turbulent Energy Budget at the Top of the Daytime Atmospheric Boundary Layer', *J. Atmos. Sci.* **34**, 111–123.

Zilitinkevich, S. S.: 1975, 'Comments on a Paper by H. Tennekes', *J. Atmos. Sci.* **32**, 991–995.

Zilitinkevich, S. S., Chalikov, D. V., and Resnyansky, Y. D.: 1979, 'Modeling the Oceanic Upper Layer', *Oceanol. Acta* **2**, 219–240.